

Title: **Structural Damage Detection Using Time Windowing Technique from Measured Acceleration during Earthquake**

Authors: Graduate Student Seung Keun Park (Presenter)
School of Civil, Urban & Geosystem Engineering
Seoul National University
San 56-1, Shillim-dong, Kwanak-gu
Seoul, 151-742, Korea
Phone: +82-2-880-8740
Fax: +82-2-887-0349
E-mail: skpark97@snu.ac.kr

Professor Hae Sung Lee
School of Civil, Urban & Geosystem Engineering
Seoul National University
San 56-1, Shillim-dong, Kwanak-gu
Seoul, 151-742, Korea
Phone: +82-2-880-8388
Fax: +82-2-887-0349
E-mail: chslee@plaza.snu.ac.kr

Structural Damage Detection Using Time Windowing Technique from Measured Acceleration during Earthquake

Seung Keun Park and Hae Sung Lee

ABSTRACT

This paper presents a system identification (SI) scheme in time domain using measured acceleration data. The error function is defined as the time integral of the least square errors between the measured acceleration and the calculated acceleration by a mathematical model. Damping parameters as well as stiffness properties of a structure are considered as system parameters. The structural damping is modeled by the Rayleigh damping. A new regularization function defined by the L_1 -norm of the first derivative of system parameters with respect to time is proposed to alleviate the ill-posed characteristics of inverse problems and to accommodate discontinuities of system parameters in time. The time window concept is proposed to trace variation of system parameters in time. Numerical simulation study is performed through a two-span continuous truss subject to ground motion.

Key Words: System Identification, Regularization, Time Window, Ground Motion

INTRODUCTION

Immediate safety assessment structures after an earthquake is extremely important in evaluating serviceability and functionality of social infrastructures. Nowadays, not only ground acceleration but also acceleration of important social infrastructures is monitored during earthquakes. It would be very helpful for quick restoration of social activities if structural damage caused by an earthquake is accessed with the measured acceleration during an earthquake in real time or near real time.

Various damage assessment schemes based on system identification (SI) have been extensively investigated for social infrastructures during the last few decades. The modal analysis approaches have been widely adopted to detect structural damage using measured acceleration of structures. The modal analysis approaches, however, suffer from drawbacks caused by insensitiveness of modal data to changes of structural properties.

To overcome the drawbacks of the modal analysis approaches, this paper presents a system identification scheme in time domain using measured acceleration data. The error function is defined as the time integral of the least square errors between the measured acceleration and the calculated acceleration by a mathematical model. The structural damping is modeled by the Rayleigh damping. A regularization technique is employed to overcome the ill-posedness of inverse problems. A regularization function defined by the L_1 -norm of first time derivatives of stiffness parameters is proposed to accommodate abrupt changes of system parameters in time. The L_1 -truncated singular value decomposition (TSVD) is adopted to optimize the error function with the L_1 -regularization function. To trace the variation of stiffness parameters in time, a time windowing technique is introduced. In the time windowing technique, SI is performed sequentially within a finite time interval, which is called a time window. The time window advances forward at each time step to identify changes of system parameters in time. As a simple case of earthquake excitation, a harmonic ground motion is applied to the example. The validity and accuracy of the proposed method are demonstrated through numerical simulation study.

PARAMETER ESTIMATION SCHEME IN TIME DOMAIN

The discretized equation of motion of a structure subjected to ground acceleration \mathbf{a}_g caused by an earthquake is expressed as follows.

$$\mathbf{M}\mathbf{a} + \mathbf{C}(\mathbf{x}_c)\mathbf{v} + \mathbf{K}(\mathbf{x}_s)\mathbf{u} = -\mathbf{M}\mathbf{a}_g \quad (1)$$

where \mathbf{M} , \mathbf{C} and \mathbf{K} represent the mass, damping and stiffness matrix of the structure, respectively, and \mathbf{a} , \mathbf{v} and \mathbf{u} are the relative acceleration, velocity and displacement of the structure to ground motion, respectively. The damping parameters and the stiffness parameters of the structure are denoted by \mathbf{x}_c and \mathbf{x}_s in (1), respectively. Newmark β -method is used to integrate the equation of motion. Since the operational vibrations of a structure are negligible compared to those induced by an earthquake, the initial condition of (1) is set to zero.

In case ground acceleration as well as accelerations of a given structure at some discrete observation points are measured, the unknown system parameters of a structure including stiffness and damping properties are identified through minimizing least squared errors between computed and measured acceleration. In case the system parameters are invariant in time, the parameter estimation procedure is represented by the following optimization problem.

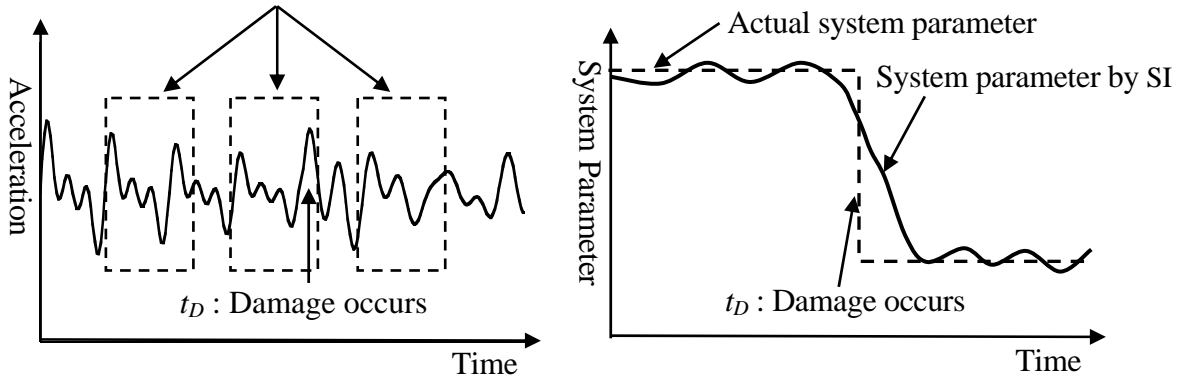


Figure 1. Time window concept

$$\text{Min}_{\mathbf{x}} \Pi_E(t) = \frac{1}{2} \int_0^t \|\tilde{\mathbf{a}}(\mathbf{x}) - \bar{\mathbf{a}}\|_2^2 dt \quad \text{subject to } \mathbf{R}(\mathbf{x}) \leq 0 \quad (2)$$

where $\tilde{\mathbf{a}}$, $\bar{\mathbf{a}}$, \mathbf{x} and \mathbf{R} are the calculated acceleration and the measured acceleration at observation points relative to ground acceleration, system parameter vector and constraint vector, respectively, with $\|\cdot\|_2$ representing the 2-norm of a vector. Linear constraints are used to set physically significant upper and lower bounds of the system parameters. The minimization problem defined in (2) is a constrained nonlinear optimization problem because the acceleration vector $\tilde{\mathbf{a}}$ is a nonlinear implicit function of the system parameters.

In case the system parameters vary with time, the time window technique is proposed. Fig.1 illustrates the time window concept. In this technique the minimization problem for the estimation of the system parameters is defined in a finite time interval, which is referred to as a time window.

$$\text{Min}_{\mathbf{x}} \Pi_E(t) = \frac{1}{2} \int_t^{t+d_w} \|\tilde{\mathbf{a}}(\mathbf{x}(t)) - \bar{\mathbf{a}}\|_2^2 dt \quad \text{subject to } \mathbf{R}(\mathbf{x}(t)) \leq 0 \quad (3)$$

Here, t and d_w is the initial time and the window size of a given time window. It is assumed that system parameters are constant in a time window, and that system parameters estimated by (3) represent the system parameters at time t . As the time window advances forward sequentially in time, the variations of system parameters in time are identified.

L_1 -REGULARIZATION SCHEME

The parameter estimation defined by the minimization problems is a type of ill-posed inverse problems. Ill-posed problems suffer from three instabilities: nonexistence of solution, non-uniqueness of solution and discontinuity of solution when measured data are polluted by noise. Because of the instabilities, the optimization problem given in (2) and (3) may yield meaningless solutions or diverge in optimization process. Attempts have been made to overcome instabilities of inverse problems merely by imposing upper and lower limits on the system parameters. However, it

has been demonstrated by several researchers that the constraints on the system parameters are not sufficient to guarantee physically meaningful and numerically stable solutions of inverse problems.

The regularization technique proposed by Tikhonov is widely employed to overcome the ill-posedness of inverse problems. In the Tikhonov regularization technique, a positive definite regularization function is added to the original optimization problem.

$$\text{Min}_{\mathbf{x}} \Pi(t) = \Pi_E(t) + \lambda \Pi_R(t) \text{ subject to } \mathbf{R}(\mathbf{x}) \leq 0 \quad (4)$$

where Π_R and λ are a regularization function and a regularization factor, respectively. Various regularization functions are used for different types of inverse problems. Kang et al proposed the following regularization function defined by the L_2 -norm for the SI in time domain.

$$\Pi_R(t) = \frac{1}{2} \int_0^t \left\| \frac{d\mathbf{x}}{dt} \right\|_2^2 dt \quad (5)$$

The regularization function defined in (5) is able to represent continuously varying system parameters in time. Since, however, the system parameters may vary abruptly (Fig.2) with time during earthquakes due to damage, a regularization function that can accommodate piecewise continuous functions in time is required to assess damage that occurs during an earthquake. To represent discontinuity of system parameters in time, this paper proposes an L_1 -regularization function of the first derivative of system parameters with respect to time.

$$\Pi_R(t) = \frac{1}{2} \int_t^{t+d_w} \left\| \frac{d\mathbf{x}}{dt} \right\|_1 dt \quad (6)$$

where $\|\cdot\|_1$ representing the 1-norm of a vector.

Since the error function is nonlinear with respect to stiffness parameters, a Newton-type optimization algorithm, which requires gradient information of an objective function, is usually

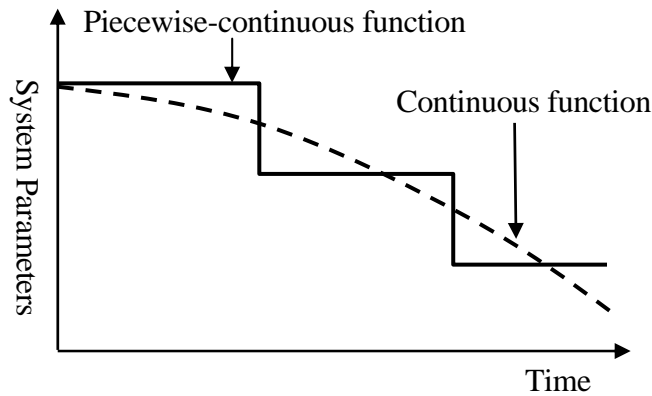


Figure 2. Continuous and piecewise-continuous function

employed in SI. As the L_1 -regularization function is non-differentiable, the objective function in the Tikhonov regularization scheme defined in (4) contains a non-differentiable function, and thus a Newton-type optimization algorithm cannot be applied. To avoid this difficulty, this paper employs the L_1 -TSVD to impose the L_1 -regularization function in the optimization of the error function. In the proposed method, the incremental solution of the error function is obtained by solving the quadratic sub-problems without the constraints. The noise-polluted solution components are truncated from the incremental solution. Finally, the regularization function is imposed to restore the truncated solution components and the constraints. The above procedure is defined as follows.

$$\text{Min}_{\mathbf{x}} \Pi_R(t) = \frac{1}{2} \int_t^{t+d_w} \left\| \frac{d\mathbf{x}}{dt} \right\|_1 dt \quad \text{subject to} \quad \mathbf{R}(\mathbf{x}) \leq 0 \quad \text{and} \quad \text{Min}_{\mathbf{x}} \Pi_E(t) = \frac{1}{2} \int_t^{t+d_w} \|\tilde{\mathbf{a}}(\mathbf{x}) - \bar{\mathbf{a}}\|_2^2 dt \quad (7)$$

The error function and the regularization function are easily discretized in time domain using simple numerical methods. The truncated solution of the minimization problem of the error function is obtained by the truncated singular value decomposition, while the simplex method is employed to solve the minimization problem of the L_1 -regularization function with constraints. Detailed solution procedures are presented in References.

DAMPING MODEL

It is a difficult task to model damping properties of real structures. In fact, existing damping models cannot describe actual damping characteristics exactly, and are approximations of real damping phenomena to some extents. Since the damping has an important effect on dynamic responses of a structure, the damping properties should be considered properly in the parameter estimation scheme. In most of previous studies on the parameter estimation, the damping properties of a structure are assumed as known properties, and only stiffness properties are identified. However, the damping properties are not known a priori and should be included in system parameters in the SI.

Among various classical damping models, the modal damping and the Rayleigh damping are the most frequently adopted model. In the modal damping, a damping matrix is constructed by using generalized modal masses and mode shapes. In Rayleigh damping, a damping matrix is defined as a linear combination of the mass matrix and stiffness matrix as follows.

$$\mathbf{C} = a_0 \mathbf{M} + a_1 \mathbf{K} \quad (8)$$

The damping coefficients of the Rayleigh damping can be determined when any two modal damping ratios and the corresponding modal frequencies are specified.

In case the modal damping is employed in the parameter estimation, the number of the system parameters associated with the damping is equal to that of the total number of DOFs, which increases the total number of unknowns in the optimization problem given in (8). Since neither modal damping nor Rayleigh damping can describe actual damping exactly, and the modal damping requires more unknowns than the Rayleigh damping in the parameter estimation, this study employs the Rayleigh damping for the SI. The Rayleigh damping yields a linear fit to the exact damping of a structure. To approximate actual damping of a structure more accurately, Caughey damping, which is the general form of the rayleigh damping, may be adopted.

$$\mathbf{C} = \mathbf{M} \sum_{i=0}^{J-1} a_i (\mathbf{M}^{-1} \mathbf{K})^i, \quad J \leq ndof \quad (9)$$

where $ndof$ is the total number of degrees of freedom of the given structure. For $J=2$, the Caughey damping becomes identical to the Rayleigh damping.

In case either the regularization scheme or damping estimation is not included in the SI, the optimization procedure does not converge or converges to meaningless solutions. Therefore, only the results with the regularization scheme and damping estimation are presented here.

EXAMPLE

Two Numerical simulation studies are presented to illustrate validity of the time windowing technique. Numerical simulation study is performed through a two-span continuous truss subject to free vibration and ground motion. The integration constants of the Newmark β -method, $\beta=1/2$, $\gamma=1/4$, are used for all cases.

Case I : Free Vibration

The validity of the proposed time windowing technique is examined through a simulation study with a two-span continuous truss shown in Fig. 3. Typical material properties of steel (Young's modulus = 210 GPa, Specific mass = $7.85 \times 10^3 \text{ Kg/m}^3$) are used for all members. The cross sectional areas of top, bottom, vertical and diagonal members are 250 cm^2 , 300 cm^2 , 200 cm^2 and 220 cm^2 , respectively. The natural frequencies of the truss range from 6.6 Hz to 114.7 Hz. Damage of the truss is simulated with 40% and 50% reductions in the sectional areas of member 7 and 16, respectively. The damaged members are depicted by dotted lines in Fig. 3. It is assumed that the damage suddenly occurs at $t=0.5$ sec. Accelerations of the truss are measured from a free vibration induced by a sudden release of applied loads of 1 KN shown in Fig. 3. The measurement errors are simulated by adding 3% random noise generated from a uniform probability function to accelerations calculated by the finite element model. The observation points are located at 12 bottom nodes of the truss. Both x- and y- direction accelerations are measured in the time period from 0 sec to 2 sec with the interval of 1/200 sec. To filter high frequency mode, the interval of inverse analysis is 1/100 sec. Fig. 7 shows the exact modal damping ratios used for the calculation of measured accelerations together with identified modal damping ratios by the Rayleigh damping. The initial modal damping ratios calculated by the assumed Rayleigh damping coefficients are also drawn in the same figure. The truncation number of the TSVD is selected as 14. The size of time window is 0.2 sec.

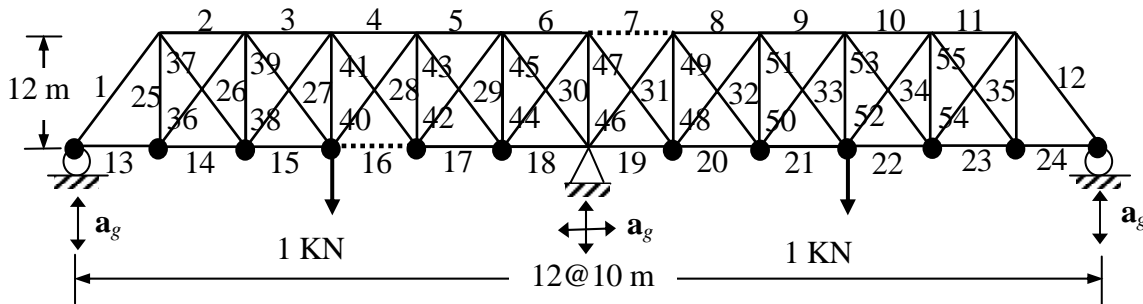


Figure 3. 2-span continuous truss

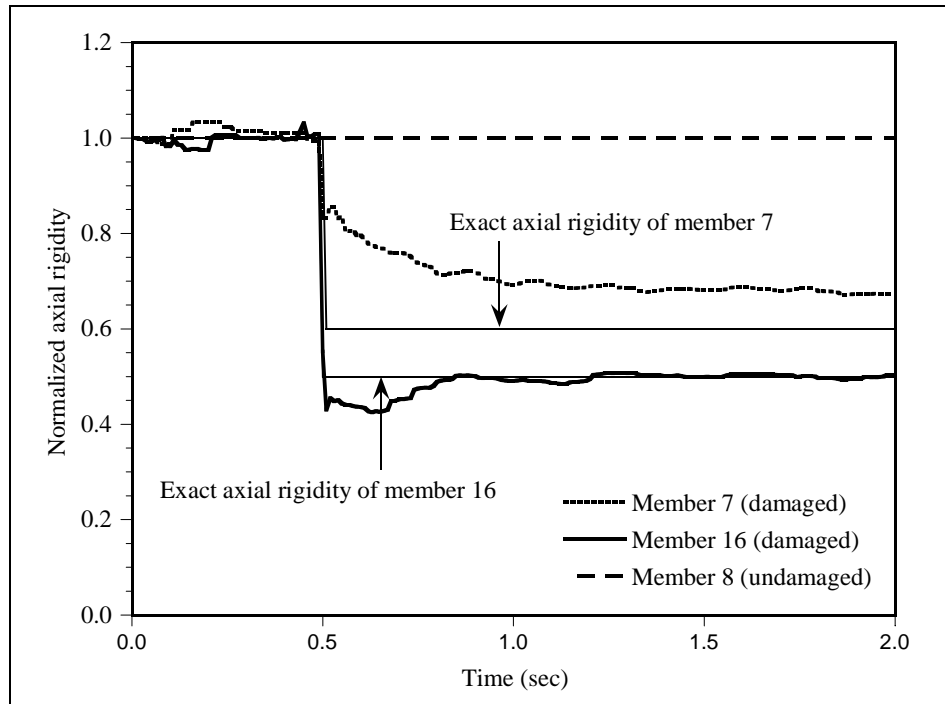


Figure 4. Variation of axial rigidities of three damaged members and one undamaged member

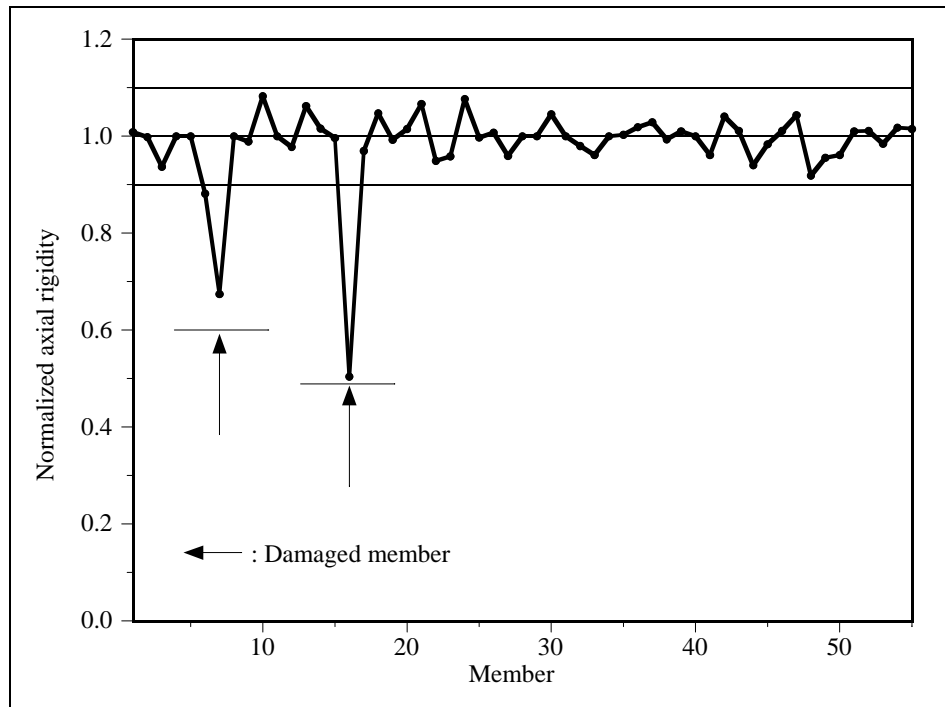


Figure 5. Identified axial rigidities at the final time step

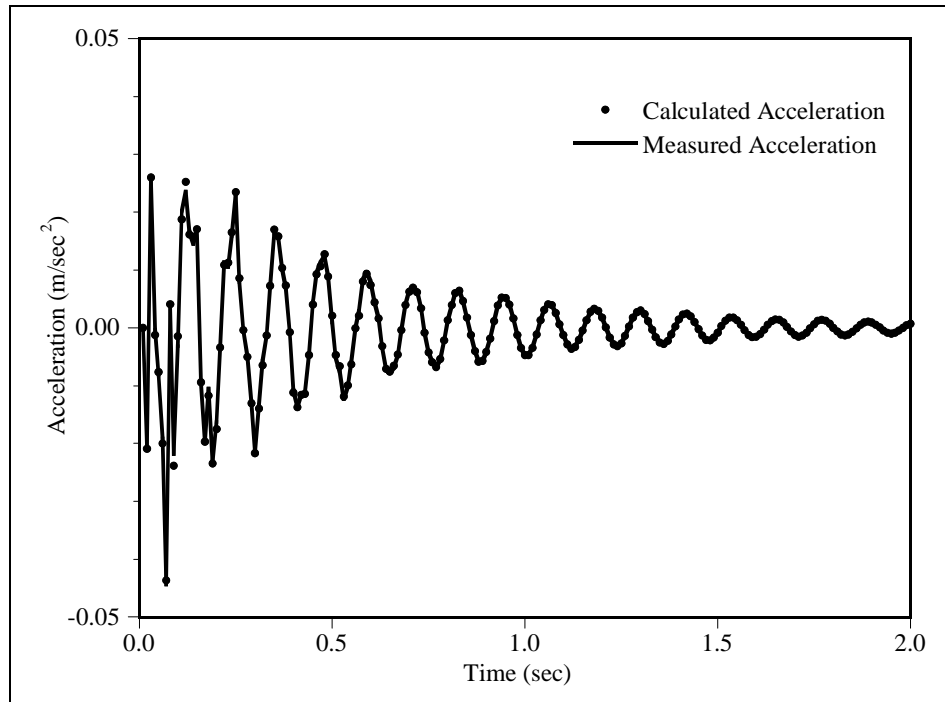


Figure 6. Measured and calculated acceleration at the center of the left span

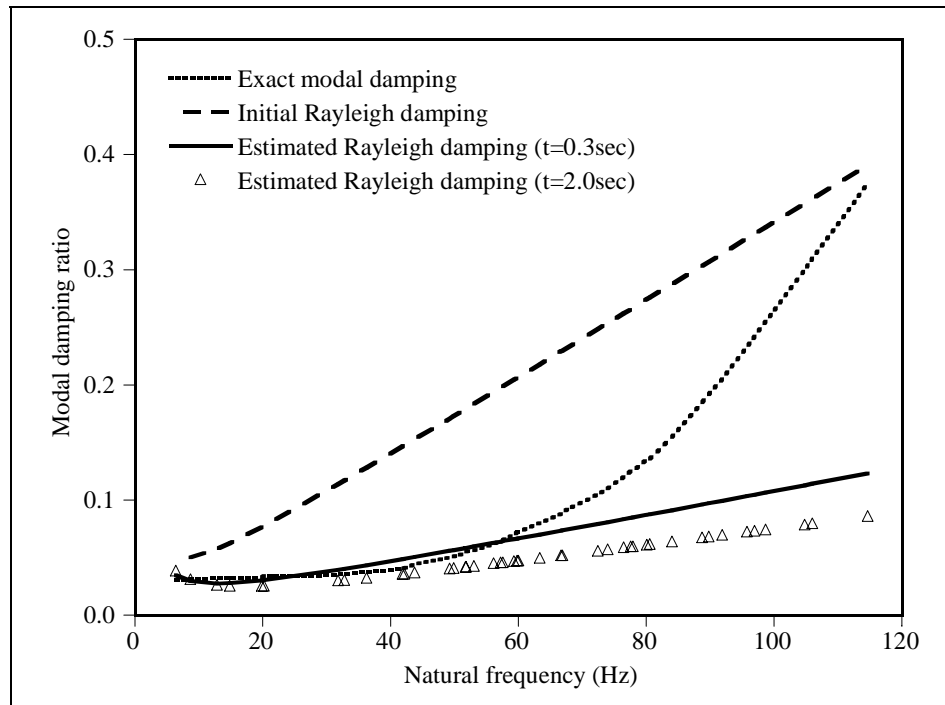


Figure 7. Identified modal damping ratios before and after the damage occurs

The variations of axial rigidities of the two damaged members and one undamaged member with time are drawn in Figure 4. From the figure, it is clearly seen that the damage occurs at $t=0.5$ sec, and that the estimated stiffness parameters of damaged members 7 and 16 converge to the actual values as time steps proceed. Figure 5 shows the axial rigidity of each member identified at the final time $t=2.0$ sec. The vertical axes of both Figure 4 and Figure 5 represent the normalized axial rigidity with respect to the initial value of each member. The identified axial rigidities oscillate moderately within the range of $\pm 10\%$ for 51 undamaged members out of 52, while the oscillation magnitudes of the other 1 undamaged members are a little higher than 10%. Since, however, axial rigidities of the damaged members are reduced prominently compared with those of the other members, the damaged members are clearly distinguished from undamaged members. Figure 6 compares the simulated acceleration with the calculated acceleration at the middle of the left span by the identified system parameters at the final time step. The calculated acceleration agrees well with the measured one.

Figure 7 shows the variations of the identified damping ratios frequency at $t=0.3$ sec (before damage) $t=2.0$ sec (after damage). The identified Rayleigh damping approximates the exact modal damping closely in the range up to 50 Hz, which corresponds to the 16th mode, while the errors in the modal ratios become larger for higher modes. Since, however, the natural frequencies corresponding to dominant lower modes are much less than 50 Hz, such approximation is good enough to identify the system parameters and to match the dynamic response correctly.

Case II : Ground Motion

In case the base undergoes ground motion, numerical simulation study is performed through a two-span continuous truss. For a fundamental investigations on the ground motion, it is assumed that the ground motion is harmonic motion $\mathbf{a}_g = A \sin \omega t$. The frequency of ground motion is 0.75 Hz. The amplitude of ground motion is 5 m/sec². Material properties of the truss are the same value as case I. Damage of the truss is simulated with 40% and 50% reductions in the sectional areas of member 7 and 16 respectively. Accelerations of the truss are measured from a vibration induced by a ground motion (Fig. 3). The measurement errors are simulated by adding 3% random noise generated from a uniform probability function to accelerations calculated by the finite element model. The observation points and directions and time are identical to case I. The interval of inverse analysis is 1/200 sec. The damping properties are the same value as case I. The truncation number of the TSVD is selected as 17. The size of time window is 0.2 sec.

The variations of axial rigidities of the two damaged members and one undamaged member with time are drawn in Figure 8. From the figure, it is clearly seen that the damage occurs at $t=0.5$ sec, and that the estimated stiffness parameters of damaged members 7 and 16 converge to the actual values as time steps proceed. Figure 9 shows the axial rigidity of each member identified at the final time $t=2.0$ sec. The vertical axes of both Figure 8 and Figure 9 represent the normalized axial rigidity with respect to the initial value of each member. The identified axial rigidities oscillate moderately within the range of $\pm 10\%$ for 49 undamaged members out of 52, while the oscillation magnitudes of the other 3 undamaged members are a little higher than 10%. Since, however, axial rigidities of the damaged members are reduced prominently compared with those of the other members, the damaged members are clearly distinguished from undamaged members. Figure 10 compares the simulated acceleration with the calculated acceleration at the middle of the left span by the identified system parameters at the final time step. The calculated acceleration agrees well with the measured one except that the time window is located in $t=0.3\sim 0.5$ sec.

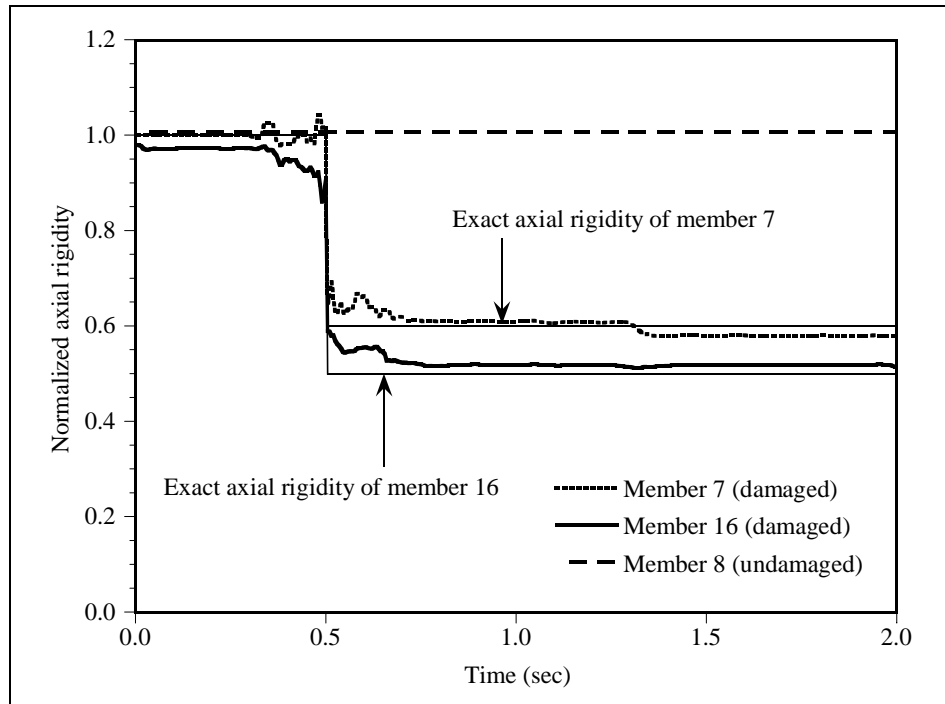


Figure 8. Variation of axial rigidities of three damaged members and one undamaged member

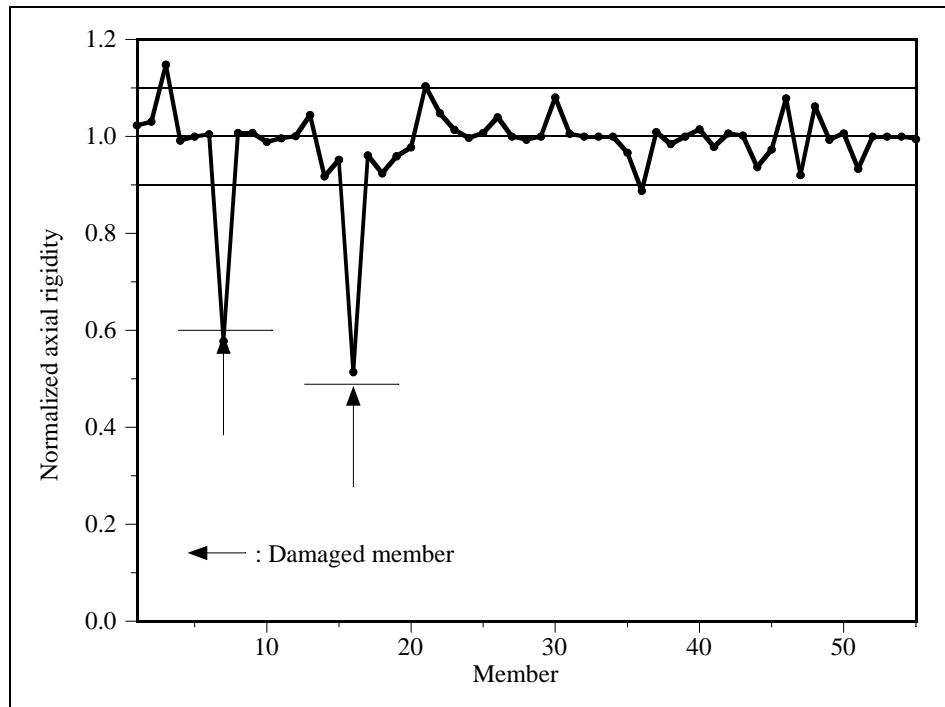


Figure 9. Identified axial rigidities at the final time step

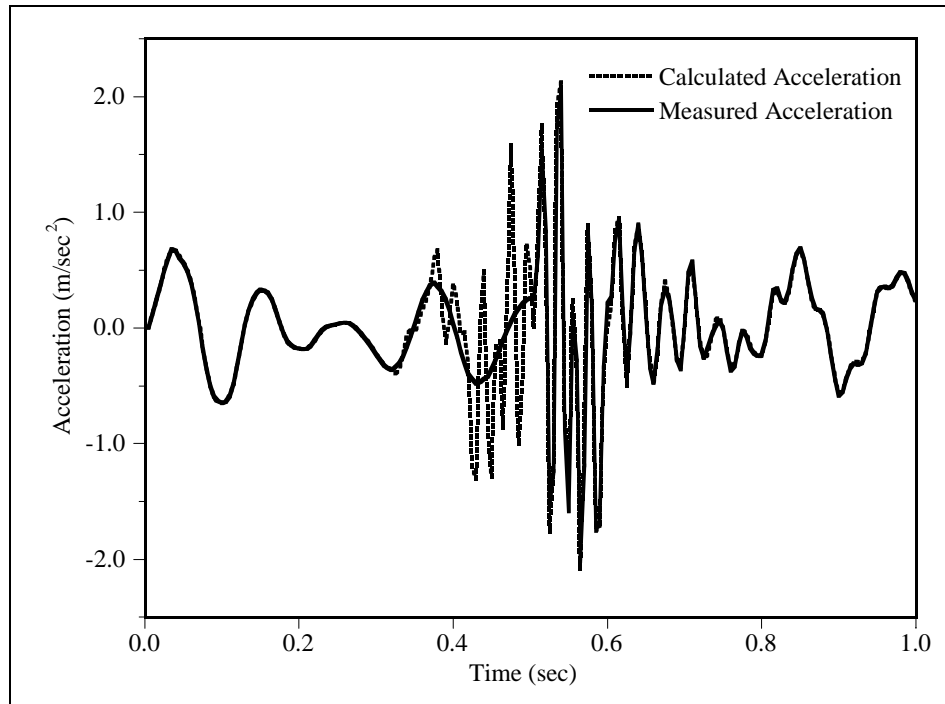


Figure 10. Measured and calculated acceleration at the center of the left span

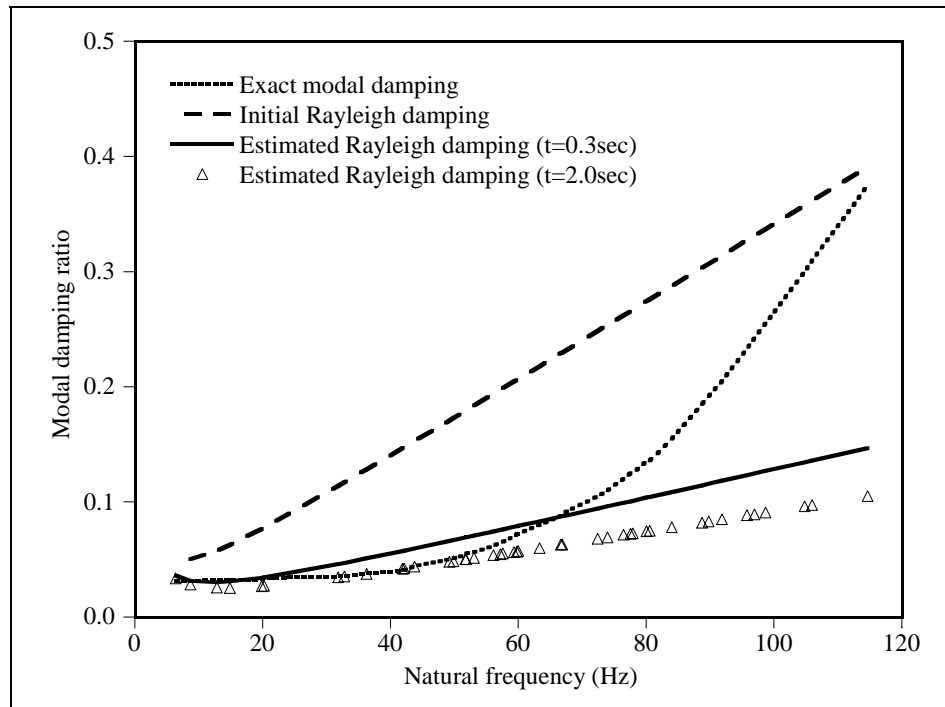


Figure 11. Identified modal damping ratios before and after the damage occurs

Figure 11 shows the variations of the identified damping ratios frequency at $t=0.3$ sec (before damage) and $t=2.0$ sec (after damage). The identified Rayleigh damping approximates the exact modal damping closely in the range up to 60 Hz, which corresponds to the 22nd mode, while the errors in the modal ratios become larger for higher modes. Since, however, the natural frequencies corresponding to dominant lower modes are much less than 60 Hz, such approximation is good enough to identify the system parameters and to match the dynamic response correctly.

CONCLUSION

The L_1 -regularization function and the time window technique are proposed for SI in time domain using measured acceleration data is proposed. The system parameters include the damping parameters as well as the stiffness parameters of a structure. The Rayleigh damping is used to estimate the damping characteristics of a structure. The least square errors of the difference between calculated acceleration and measured acceleration is adopted as an error function. The regularization technique is employed to alleviate the ill-posedness of the inverse problem in SI. The L_1 -TSVD is utilized to optimize a non-differential object function.

The proposed method exhibits very compromising characteristics in detecting damage, and is able to estimate the stiffness properties accurately even though the damping characteristics are approximated by the Rayleigh damping. The example presented in this paper shows capabilities of the time window technique for the identification of damage caused by earthquakes.

REFERENCES

- Yeo, I. H., Shin, S. B., Lee, H. S. and Chang, S. P., Statistical damage assessment of framed structures from static responses, *Journal of Engineering Mechanics*, ASCE, Vol. 126, No. 4, pp. 414-421, 2000
- Shi, Z.Y., Law, S.S. and Zhang, L.M., Damage localization by directly using incomplete mode shapes, *Journal of Engineering Mechanics*, ASCE, Vol. 126, No. 6, pp. 656-660, 2000
- Vestouni, F. and Capecchi, D., Damage detection in beam structures based on frequency measurements, *Journal of Engineering Mechanics*, ASCE, Vol. 126, No. 7, pp. 761-768, 2000
- Kang, J.S., Yeo, I.H. and Lee, H.S., Structural damage detection algorithm from measured acceleration, *Proceeding of KEERC-MAE Joint Seminar on Risk Mitigation for Regions of Moderate Seismicity*, pp. 79-86, 2001
- Hansen, P.C., *Rank-deficient and discrete ill-posed problems : Numerical aspects of linear inversion*, SIAM, Philadelphia, 1998
- Hansen, P. C., and Mosegaard, K. Piecewise polynomial solutions without a priori break points, *Numerical Linear Algebra with Applications*, Vol. 3, 513-524, 1996
- Chopra, A.K., *Dynamics of Structures (theory and applications to earthquake engineering)*, Prentice Hall, 1995.